Drilled alternating-layer structure for three-dimensional photonic crystals with a full band gap

Eiichi Kuramochi,[a] Masaya Notomi, and Toshiaki Tamamura[b]
NTT Basic Research Laboratories, 3-1 Morinosato Wakamiya, Atsugi-shi 243-0198, Japan

Takayuki Kawashima[c] and Shojiro Kawakami[c]
Research Institute of Electrical Communication, Tohoku University, Katahira 2-1-1, Aoba-ku, Sendai 980-8577, Japan

Jun-ichi Takahashi and Chiharu Takahashi
NTT Telecommunications Energy Laboratories, 3-1 Morinosato Wakamiya, Atsugi-shi 243-0198, Japan

(Received 1 June 2000; accepted 25 August 2000)

A new three-dimensional photonic crystal structure is designed to simplify fabrication. A calculation of the band structure predicts that this photonic crystal has a complete photonic band gap in all directions. The entire three-dimensional periodic structure, except for the vertically drilled holes, is formed by automatic shaping during bias sputtering deposition. The fabrication technologies used to construct this photonic crystal are electron beam lithography, bias sputtering, and fluoride-gas electron cyclotron resonance etching. Our preliminary fabrication reveals that each technology can be controlled well enough to lead to the creation of a photonic band gap material for an optical communication wavelength. © *2000 American Vacuum Society.* [S0734-211X(00)07806-9]

I. INTRODUCTION

A three-dimensional (3D) photonic crystal (PC) can possess a full photonic band gap (PBG).[1] We can control the propagation or radiation of light inside a solid by using PBG material. Therefore, PCs are expected to lead to a new class of photonic components.[1] A PC waveguide made by 3D PC has been reported[2] which will allow miniaturized photonic circuits to be developed. However, constructing a 3D PC is still very difficult. The major problem is that current lithography techniques are not suitable for vertical nanofabrication of a 3D PC. For example, the woodpile-type 3D PC (Refs. 2–4) requires layer-by-layer fabrication, which increases the process steps, or a micromachining technique, which is very complicated. Yablonovite,[5] which is constructed by drilling at three different angles, is a superior crystal structure in the microwave range. However, drilling cylindrical holes that intersect each other is very difficult in the visible or near-infrared range where the hole radius is micron to submicron. Very recently, a simple cubic PC constructed by combining vertical drilling with selective etching has been reported,[6] but the low controllability of selective etching limits the PBG wavelength range.

Therefore, 3D-PCs, which can be constructed with fewer process steps without sophisticated technology, are expected to be developed. The 3D PC proposed by Fan *et al.*[7] is noteworthy because it can be constructed by a planar lithography process, although it still needs layer-by-layer patterning. An alternating-layer structure can be constructed very simply. Recently, Kawakami and co-workers found that 3D or two-dimensional (2D) alternating-layer PCs can be constructed by bias sputtering under automatic shaping conditions.[8,9] However, an alternating-layer structure itself cannot possess a PBG due to the lack of z connectivity.

In this article we report a new 3D PC structure that requires very few process steps and can open a large PBG. Although very precise nanofabrication is still required, the fabrication technologies used in this work have already been used in industry, so they are practical. Some preliminary fabrication results are presented.

II. PHOTONIC CRYSTAL DESIGN

The underlying idea of our design concept is to construct a PC by combining alternating-layer film deposition with as few nanofabrication steps as possible. The expected outcome, which we call the drilled alternating-layer photonic crystal (DALPC), is shown in Fig. 1. The DALPC consists of alternating layers with periodical corrugation and a 2D array of cylindrical columns made by vertical drilling. Since the periodically corrugated alternating-layer structure is a 2D photonic crystal,[10] we refer to it as 2D-ALPC hereafter. The DALPC is geometrically similar to a diamond structure, which is similar to the woodpile-type structure,[2–4] so that it should have a full PBG.

Figure 2 shows the DALPC photonic band structure calculated by the plane wave expansion method, where the lattice constants are $L_x = a$ and $L_y = L_z = 0.7a$, and the air hole radius is $r = 0.23a$. Figure 3 shows a PBG that is 12% of the midgap frequency in all directions. In this work, 2D-ALPCs were made only from Si/SiO_2 and the cylindrical columns were restricted to air holes.

[a]Electronic-mail: kuramoti@will.brl.ntt.co.jp
[b]Present address: NTT Electronics Corporation, 3-1 Morinosato Wakamiya, Atsugi-shi 243-0198, Japan.
[c]Present address: New Industry Creation Hatchery Center, Tohoku University, Aramaki-Aza-Aoba, Aoba-ku, Sendai 980-8579, Japan.

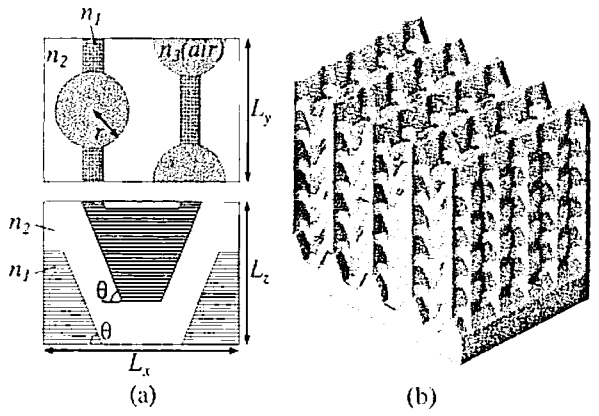

FIG. 1. Schematics of the DALPC structure. (a) Plane views (top/side) of a unit cell. Alternating layers are dielectric materials with refractive indexes n_1 and n_2. The refractive index of the cylindrical columns, n_3, is regarded as 1 (air). The angle of the slope of periodical corrugation, θ, is constant. (b) A bird's eye view.

III. EXPERIMENT

Figure 3 shows the DALPC process which consists of five steps. First, electron beam (EB) lithography is used to define a set of periodic grooves which serve as the template for the 2D-ALPC [Fig. 3(a)]. ZEP520 resist (Nippon Zeon) is patterned as the etching mask for the grooves. Alignment marks made of Ni are placed around the PC patterns before the grooves are formed. The marks are referenced to achieve high positional accuracy in every lithography step. The grooves are then etched by conventional reactive ion etching (RIE). Second, a 2D-ALPC consisting of Si/SiO_2 multilayers is deposited onto the patterned substrate by rf-bias sputtering after the removal of resist masks [Fig. 3(b)]. Corrugation of the alternating layers is achieved by the automatic shaping effect in bias sputtering triggered by the periodic grooves on the substrate. Since bias sputtering combines sputter deposition with sputter etching, the balance between these two processes determines surface shape. At an appropriate sputter condition, surface corrugation is stabilized and maintained throughout the bias sputtering. The whole 2D-ALPC can be constructed by bias sputtering under automatic shaping conditions in a deposition sequence, which requires only one

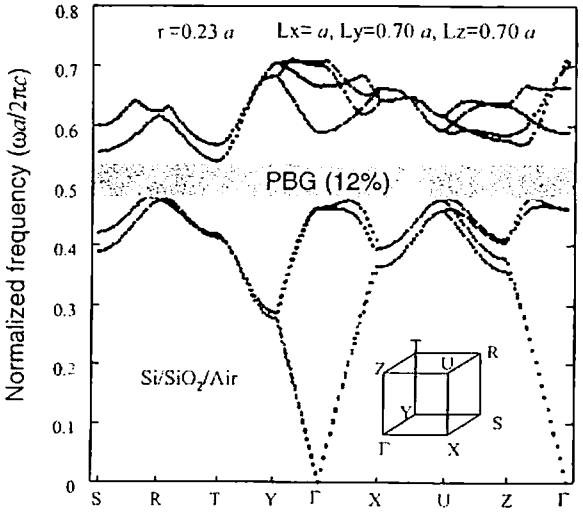

FIG. 2. Calculated photonic band diagram of a DALPC model. The PBG is 12% of the midgap frequency (shaded area).

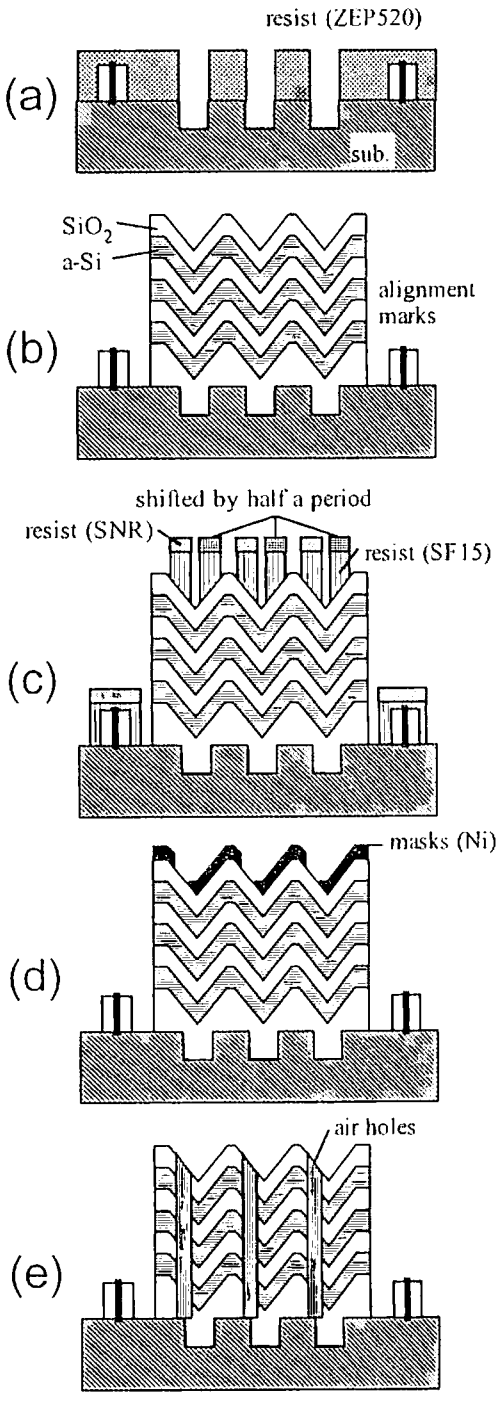

FIG. 3. Process sequence of DALPC fabrication. (a) Fabrication of periodic grooves on a substrate by lithography. (b) Deposition of 2D-ALPC by rf-bias sputtering under automatic shaping conditions after resist removal. (c) EB exposure and development of a bilayer resist system for the lift-off process. (d) Lift-off of Ni etching masks after evaporation. (e) Drilling of cylindrical columns by dry etching, and removal of the Ni mask by HCl solution.

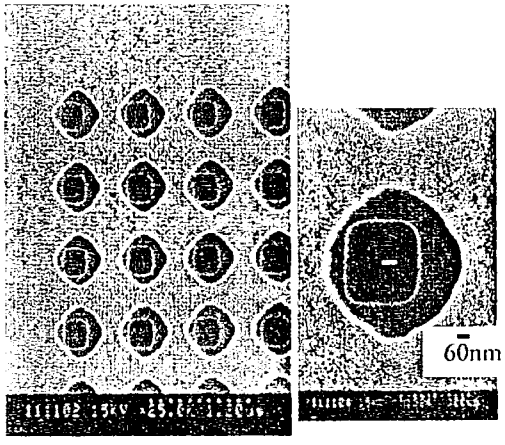

FIG. 4. SEM images of doubly patterned holes. The shift between two patterns corresponds to the alignment error in the EB exposing machine.

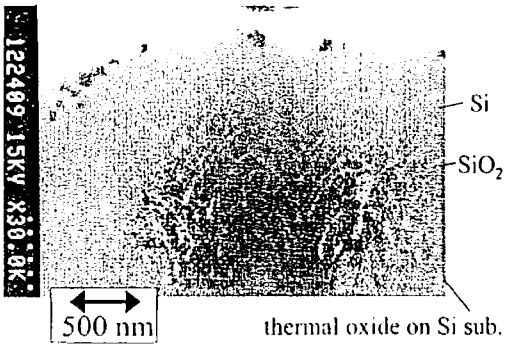

FIG. 5. Cross-sectional SEM image of a Si/SiO_2 2D-ALPC deposited by autocloning.

lithography step. This is the most significant difference between our DALPC and the PC proposed by Fan *et al.*[7] Then, the Ni patterns, which act as etching masks for dry etching into the alternating Si/SiO_2 layers to fabricate air holes, are prepared by a conventional lift-off technique. As shown in Fig. 3(c), the third process is patterning SNR[11]/PMGI (MicroChem) bilayer resist for lift-off. The SNR resist is very thin and has extremely high selectivity for O_2 RIE. Here, a second EB lithography step is conducted by referring to the alignment marks. After developing the SNR resists, the patterns are transferred to the PMGI layer by O_2 RIE. Next, the Ni film is evaporated and then unnecessary Ni is lifted off along with underlying PMGI resist by soaking in Microposit remover 1165 (Shipley), as shown in Fig. 3(d). Finally, the air holes are drilled by electron cyclotron resonance (ECR) etching [Fig. 3(e)]. Noteworthy is the fact that only two lithography steps are required in the sequence.

For EB lithography we used a 25 kV Gaussian electron beam machine (JEOL JBX-5FE), which can provide patterns with very fine pitch of less than 75 nm.[12] Since the size of a unit cell of PC is much larger than this, the fineness of the pattern is not such a serious problem. The serious issue in fabricating the DALPC is the unintentional position shift that can occur between the 2D-ALPC and drilled air holes, because it causes the PBG to narrow or disappear. In this work, the shift completely depended on the alignment accuracy of the EB exposing machine. Figure 4 shows a result of a duplicated patterning test by EB lithography, which directly indicates the alignment error. The alignment accuracy of our EB machine obtained by the tests is usually 50–90 nm when alignment marks placed around the patterns are detected (direct drawing mode). We consider an alignment error of about 50 nm to be acceptable for DALPC with $a = 700$ nm, which corresponds to a PBG center wavelength of 1.5 μm. Since reference mark detection is a standard function of our EB machine, it is not necessary to use sophisticated alignment techniques.

Details of the rf-bias sputtering with automatic shaping is described elsewhere[9] which also demonstrated that the bias sputtering process with automatic shaping, called autocloning, can be represented exactly by process simulation. This means that the autocloning process is highly controllable and reproducible. Furthermore, autocloning can easily construct a 2D-ALPC comprising more than 40 pairs in the vertical direction.

We used ECR etching to drill high-aspect-ratio air holes in the DALPC. In high-aspect-ratio etching, both anisotropy and selectivity must be improved greatly. When ECR etching is carried out at gas pressures of 3×10^{-2} Pa or less, the controllability of the Si etched shape is significantly improved. Fluorinated gas containing carbon enables highly anisotropic etching of Si without rf bias.[13] In this experiment, Ni was used as the etching mask because it is hardly etched at all in reactive plasma of fluorinated gas. In order to obtain high selectivity of both Si and SiO_2 for the Ni etching mask, we used low-power rf bias conditions under which SiO_2 can be etched at almost the same rate as Si.

IV. FABRICATION RESULTS

Several sets of DALPC ($a = L_1 = 0.7\,\mu$m, $L_2 = 0.5\,\mu$m, and $L_3 = 0.3\,\mu$m) were fabricated on Si substrates on which a 1-μm-thick thermal oxide layer was formed. First, periodic grooves with 700 nm pitch and 280 nm depth were fabricated by EB lithography and C_2F_6 RIE. Then, six pairs of 200-nm-thick a-Si and 120-nm-thick SiO_2 were deposited by bias sputtering under autocloning conditions.[9] Figure 5 shows a cross section of a Si/SiO_2 2D-ALPC observed with a scanning electron microscope (SEM). It shows that the original rectangular shape changed into a zigzag shape in the early stage of deposition, and this shape was precisely maintained throughout the deposition. Although this shape did not reproduce that in Fig. 1(a) accurately, we expect that the shape will be improved by optimizing the autocloning parameters.

The ECR etching conditions under which air holes 0.25–0.3 μm in diameter are drilled into the Si/SiO_2 multilayer film were examined using a SF_6–CF_4–CO_2 gas mixture and 400 kHz rf bias. At low gas pressure, 400 kHz rf bias can accelerate ions for SiO_2 etching without increasing the number of fluorine radicals that cause Si undercut. Figure 6 shows the CF_4 flow rate ratio dependence and rf power de-

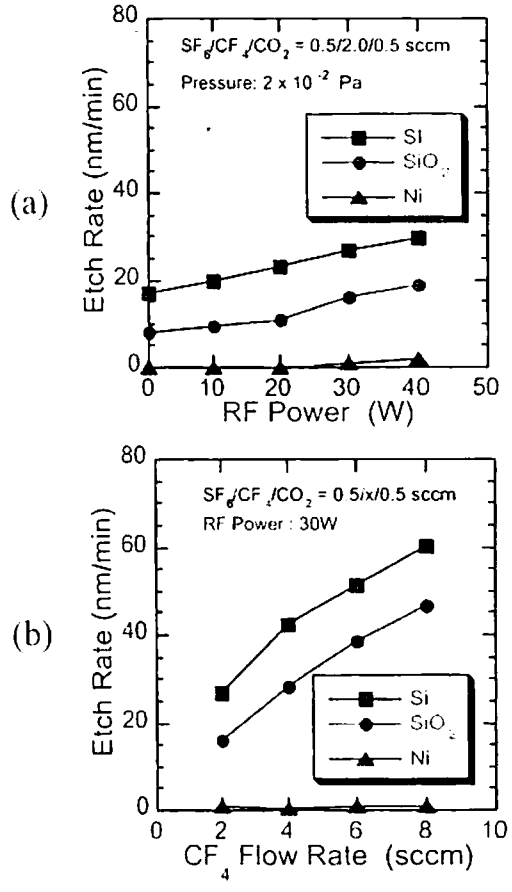

FIG. 6. Si and SiO_2 etching characteristics when ECR etching with a SF_6–CF_4–CO_2 mixture is carried out at low rf powers (a) rf power dependence; (b) flow rate dependence. The microwave power is 400 W.

pendence of the etching characteristics. For all etching conditions, Si undercut is strongly suppressed by the carbon component generated by decomposing CF_4 in high-density ECR plasma. In Fig. 6(a), the SiO_2 etch rate increases more than Si etch rate by increasing rf power. In Fig. 6(b), the SiO_2 etch rate can increase to 70% of the value of the Si etch rate when the rf power and CF_4 flow rate are set at 30 W and 6 sccm, respectively. For these etching conditions, the etching selectivity for the Ni mask is still high, larger than 40, although the rf bias makes the Ni etch rate high due to sputtering effects.

The Ni mask lifted off from the Si/SiO_2 DALPC by EB lithography was 100 nm thick. Then, air holes were drilled by using the ECR etching with SF_6–CF_4–CO_2 at 30 W rf bias and 6 sccm CF_4 flow rate. In the drilling of DALPC with $a = 700$ nm, the diameter of the air holes was about 300 nm. Figure 7 shows a cross-sectional SEM image of a sample after drilling to a depth of about 1 μm. Air holes are successfully drilled for a practical zigzag Si/SiO_2 multilayer sample (not a flat sample). The holes are almost straight without any undercutting of the Si layer. They are also exactly positioned at the center of the slope of the zigzag patterns. The image also indicates that the alignment error between the 2D-ALPC and the air holes was less than 50 nm.

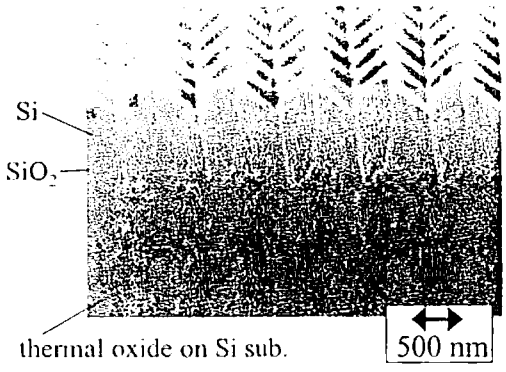

FIG. 7. Cross-sectional SEM image of a Si/SiO_2 DALPC sample after drilling by fluoride-based ECR etching.

As mentioned above, the alignment accuracy of our EB machine is about 50 nm; the reduced alignment error was achieved by introducing an intentional shift to cancel the error.

V. SUMMARY

We have proposed a drilled alternating-layer photonic crystal structure as a 3D PC. A band calculation shows the DALPC can possess a wide complete photonic band gap. The DALPC is designed to be constructed using a simple process with very few steps which is compatible with the process currently used for commercial device fabrication. We have demonstrated a preliminary result of DALPC fabrication using EB lithography, autocloning, and drilling with ECR etching.

ACKNOWLEDGMENTS

The authors thank Daisuke Takagi and Dr. Akira Ozawa for sample preparation, and Tetsuyoshi Ishii for his advice on EB lithography. They also thank Dr. Itaru Yokohama and Dr. Hideaki Takayanagi for their continuous encouragement.

[1]J. D. Joannopoulos, R. D. Meade, and J. N. Winn, *Photonic Crystals* (Princeton University Press, Princeton, NJ, 1996).
[2]S. Noda, International Workshop on Photonic and Electromagnetic Crystal Structures, Sendai, Japan, 8–10 March 2000.
[3]K. M. Ho, C. T. Chan, C. M. Soukoulis, R. Biswas, and M. Sigalas, Solid State Commun. 89, 413 (1994).
[4]H. S. Sözüer and J. P. Dowling, J. Mod. Opt. 41, 231 (1994).
[5]E. Yablonovitch, T. J. Gmitter, and K. M. Leung, Phys. Rev. Lett. 67, 2295 (1991).
[6]L. Zavich and T. S. Mayer, Appl. Phys. Lett. 75, 2533 (1999).
[7]S. Fan, P. R. Villeneuve, R. D. Meade, and J. D. Joannopoulos, Appl. Phys. Lett. 65, 1466 (1994).
[8]S. Kawakami, Electron. Lett. 33, 1260 (1997).
[9]S. Kawakami, T. Kawashima, and T. Sato, Appl. Phys. Lett. 74, 463 (1999).
[10]Y. Ohtera, T. Sato, T. Kawashima, T. Tamamura, and S. Kawakami, Electron. Lett. 35, 1271 (1999).
[11]M. Morita, S. Imamura, A. Tanaka, and T. Tamamura, J. Electrochem. Soc. 131, 2402 (1984).
[12]T. Ishii, H. Tanaka, E. Kuramochi, and T. Tamamura, Jpn. J. Appl. Phys., Part 1 37, 7202 (1998).
[13]C. Takahashi, Y. Jin, K. Nishimura, and S. Matsuo, Jpn. J. Appl. Phys., Part 1 39, 3672 (2000).